One-dimensional fragments of fullerene C_{60} that exhibit robustness toward multi-electron reduction and pronounced light absorption

Masahiro Hayakawa,[1,2,†] Naoyuki Sunayama,[3,†] Shu I. Takagi,[3] Asuka Tamaki,[2] Shigehiro Yamaguchi,[2,4] and Aiko Fukazawa*[1]

† Equal contribution

1. Institute for Integrated Cell-Material Sciences (WPI-iCeMS), Institute for Advanced Study, Kyoto University, Yoshida, Sakyo-ku, Kyoto 606-8501, Japan
2. Department of Chemistry, Graduate School of Science, and Integrated Research Consortium on Chemical Science (IRCCS), Nagoya University, Furo, Chikusa, Nagoya 464-8602, Japan
3. Department of Energy and Hydrocarbon Chemistry, Graduate School of Engineering, Kyoto University, Yoshida, Sakyo-ku, Kyoto 606-8501, Japan
4. Institute of Transformative Bio-Molecules (WPI-ITbM), Nagoya University, Furo, Chikusa, Nagoya 464-8601, Japan

*E-mail address for correspondence: afukazawa@icems.kyoto-u.ac.jp

Abstract

Fullerenes are compelling molecular materials owing to their exceptional robustness toward multi-electron reduction. Although scientists have attempted to address this feature by synthesizing various fragment molecules, the origin of this electron affinity remains unclear. Several structural factors have been suggested, including high symmetry, curved structures, and five-membered ring substructures. To elucidate the role of the five-membered ring substructures without the influence of high symmetry and curved structure, we herein report the synthesis and electron-accepting properties of oligo(biindenylidene)s, a one-dimensional fragment of fullerene C_{60}. Electrochemical studies corroborated that oligo(biindenylidene)s accept electrons equal to the number of five-membered rings in their main chains. Moreover, ultraviolet/visible/near-infrared absorption spectroscopy revealed that oligo(biindenylidene)s exhibit significantly enhanced absorption covering the entire visible region in relation to C_{60}. These results highlight the significance of the pentagonal substructure for attaining stability toward multi-electron reduction and provide a new strategy for the molecular design of electron-accepting π-conjugated hydrocarbons.

Fullerenes have fascinated scientists in broad research fields since the discovery of buckminsterfullerene C_{60}.[1] In addition to the attractive spherical structure with high symmetry, their electron-accepting characteristic is notable among π-conjugated materials. Fullerenes have exceptional stability toward multi-electron reduction, unlike other electron-accepting π-conjugated systems.[2,3] For example, C_{60} reportedly undergoes 6-electron and 12-electron

reductions in solution[2] and the solid states, respectively.[3] This robustness toward multi-electron reduction enables access to various alkaline metal salts, among which Cs_3C_{60} exhibits superconductivity with the transition temperature (T_c) of 38 K, which is the highest value among all the molecular materials.[4–6] Moreover, their moderately low-lying lowest unoccupied molecular orbital (LUMO)[7–9] and high electron mobility[10,11] have rendered them a central role as electron-transporting materials.[12] It is remarkable that this high electron affinity is realized based on the carbon-only framework. This is unlike the molecular design of most electron-accepting organic materials, which relies on introducing electron-withdrawing atoms or groups, such as fluorine,[13–15] chlorine,[14] cyano,[16–18] carbonyl,[17–19] and imine moieties,[17,19] into π-conjugated systems.

Hence, the minimum structural basis for the high electron affinity and exceptional stability toward the multi-electron reduction of fullerenes are of interest. Several structural factors have been proposed, including the degeneracy of LUMO and LUMO+1 due to the highly symmetrical structure, the mitigation of bond angle strain around the carbon atoms upon reduction due to the inherently curved structure, and the presence of five-membered ring substructures (Fig. 1a).[8,20–21] Although π-conjugated hydrocarbons with fragment structures of fullerenes can be promising for understanding the effect of each factor, most fullerene fragment molecules reported to date, such as corannulene[22,23] and sumanene,[24] as well as larger molecules[25–30] have bowl-shaped structures (Supplementary Fig. 1). This fact indicates that the curved structure of the fullerenes is of significant interest. Although Brunetti and coworkers reported π-extended 9,9′-bifluorenylidene derivatives composed of a C_{60} substructure without curvature,[31] their highly twisted structures impede the effective extension of the π-conjugation, limiting the contribution of five-membered rings. A fragment molecule with effective π-conjugation between the five-membered ring substructures similar to that of C_{60} without a curved structure is necessary to clarify the role of five-membered rings on the high electron affinity and robustness toward multi-electron reduction of fullerenes.

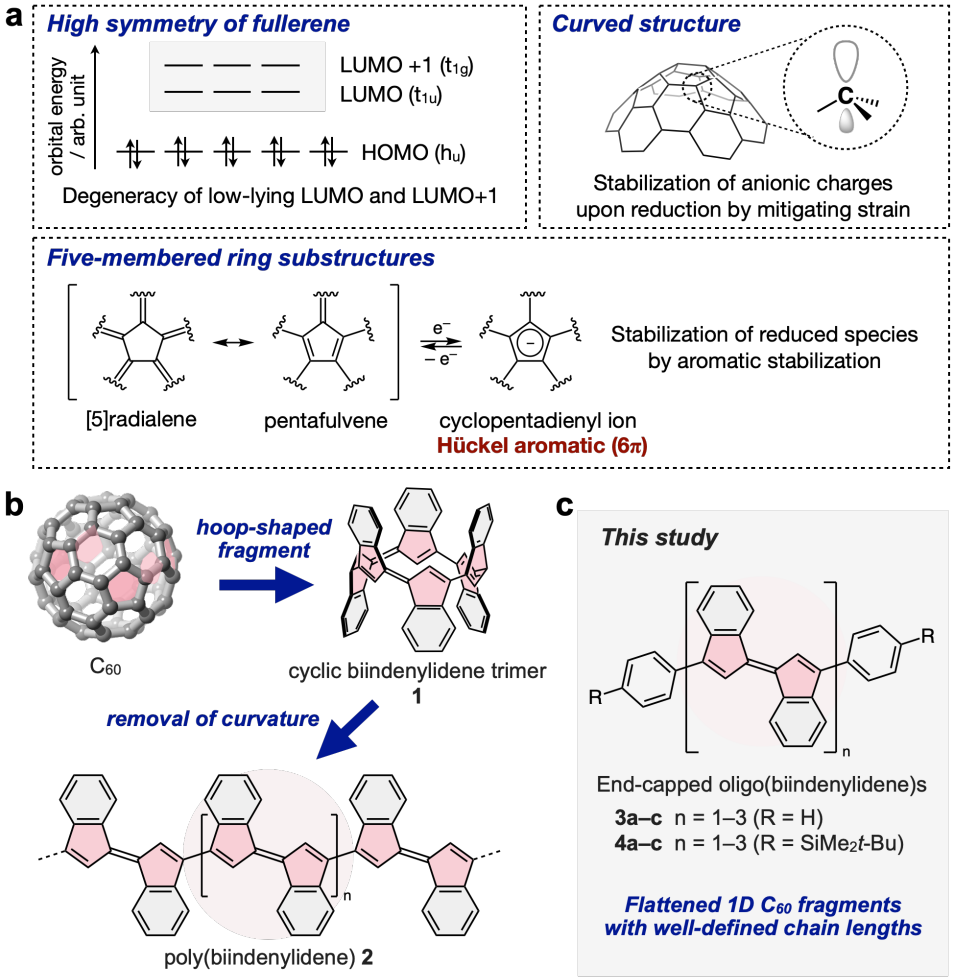

Fig. 1. Origin of prominent electron-accepting character of fullerenes. **a.** Three proposed structural factors for the electron-accepting character of fullerenes. **b.** Our molecular design of π-conjugated polymer **2** based on the hoop-shaped substructure **1** of C_{60}. **c.** End-capped oligo(biindenylidene)s **3** and **4** examined in this study.

Therefore, to elucidate the role of the five-membered ring substructures in the exceptional electron affinity of fullerenes without the influence of high symmetry and curved structure, we conceived a molecular design of π-conjugated oligomers **3** and **4** composed of a one-dimensional fragment of C_{60} in their main chains (Fig. 1c) based on the following idea. First, we focused on the hoop-shaped substructure of C_{60} wherein 6 five-membered rings were linearly connected, that is, cyclic ter(1,1′-biindenylidene) **1** (Fig. 1b). Next, based on the similarity of the π-conjugated hoops and corresponding linear π-conjugated polymers, excluding their symmetry and structural distortion,[32,33] we designed linear π-conjugated polymer **2** with an identical repeating unit to eliminate the curvature effect. We also anticipated that it could be an excellent platform for demonstrating the effect of five-membered rings on the stability toward the multi-electron reduction as the number of five-membered rings per

molecule can be increased by elongating the chain length. Poly(pentafulvalene)s, including **2**, have previously been studied as candidate structures for narrow- or zero-bandgap polymers by quantum chemical calculations[34–37] although their electron-accepting characteristics have not yet been discussed. Moreover, the synthesis of π-conjugated oligomers or polymers of pentafulvalenes has not yet been reported. In this study, to clarify the molecular structures and chain-length dependence of the properties, we designed **3** and **4**, wherein both ends of the one-dimensional C_{60} fragment (**2**) were end-capped with phenyl and 4-silylphenyl groups, respectively (Fig. 1c). Herein, we report the syntheses and properties of **3** and **4** up to n = 3. X-ray crystallographic analyses showed that the C_{60} fragment structures in **3** and **4** were unaffected by the pyramidalization of carbon atoms. Electrochemical and photophysical studies revealed the role of five-membered rings in the exceptional electron-accepting characteristic of C_{60} without electron-withdrawing groups. Moreover, comparison of the electronic structures of **3** and **4** with those of C_{60} revealed the characteristics of oligo(biindenylidene)s, reflecting one-dimensional π-conjugation between the five-membered rings.

Results and discussion

Synthesis and characterization. Oligo(1,1′-biindenylidene)s **3** and **4** were synthesized by iterative cross-coupling reactions using 3,3′-dibromo-1,1′-biindenylidene (**5**)[38,39] as a precursor. Initially, we attempted synthesizing monoarylated 1,1′-biindenylidenes (**6a** and **7a**) as end-capping building blocks by Pd-catalyzed Negishi coupling of dibromide **5** with arylzinc chloride (Fig. 2, top). However, careful separation of the products provided the expected cross-coupling products, such as monophenylated biindenylidene **6a** (15% yield) and diphenylated biindenylidene **3a** (4% yield), and the monophenylated biindenylidene dimer (**6b**, 1% yield), diphenylated biindenylidene dimer (**3b**, 1% yield), and trimer (**3c**, 0.9% yield). The reaction using trialkylsilyl-substituted phenylzinc chloride gave results identical to those described above, and the corresponding oligo(biindenylidene)s with silyl groups at both terminals (**4a**–**c**) were obtained (Fig. 2, top). Conversely, trimers **3c** and **4c** were obtained in improved yields of 59% and 45%, respectively, by the Suzuki–Miyaura coupling of organoboronate **8**, which was prepared by Pd-catalyzed borylation of **5** (Fig. 2, bottom) with **6a** and **7a**.

The molecular structures of oligo(biindenylidene)s **3a**–**c** and **4a**–**c** obtained were verified by nuclear magnetic resonance (NMR) and mass spectroscopy, and those of the monomers (**3a** and **4a**) and dimers (**3b** and **4b**) were confirmed by single-crystal X-ray diffraction analyses (Fig. 3 and Supplementary Fig. 2, *vide infra*). Notably, **3a**–**c** and **4a**–**c** were stable under ambient

conditions and could be handled without any precautions. Furthermore, a series of oligo(biindenylidene)s exhibited moderate solubility in common organic solvents. For example, the solubilities of **3b** and **3c** in CH_2Cl_2 were 5 and 2 g L^{-1}, respectively, which are one order of magnitude higher than that of C_{60} (0.26 g L^{-1}).[40]

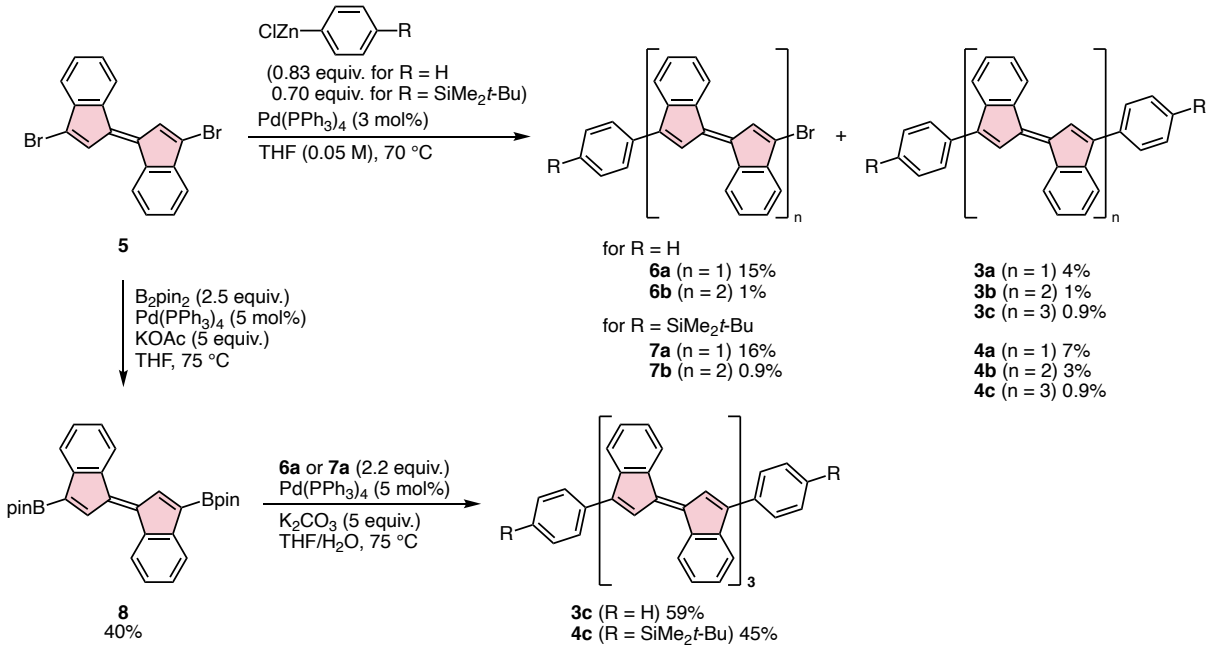

Fig. 2. Synthesis of biindenylidene oligomers.

Single-crystal X-ray diffraction analyses of **3b** and **4b** revealed one-dimensional π-conjugated frameworks wherein the biindenylidene units were directly bonded with the same connectivity as those in C_{60} (Fig. 3a and b). Each biindenylidene unit had an *E* configuration, and all the adjacent units adopted *s*-trans conformation. The C–C bond lengths in the biindenylidene units of **3b** and **4b** were comparable to those of the corresponding **3a** and **4a** without any noticeable dimerization effect (Supplementary Table 1). Although their π-conjugated frameworks deviated from coplanarity, the conformation differed depending on the terminal substituents. In particular, the biindenylidene skeletons in phenyl-capped **3b** and trialkylsilylphenyl-capped **4b** were slightly twisted to comparable extents, with intra-unit torsion angles (C2–C1–C10–C11) of 160.6° and –166.4°, respectively, because of the steric repulsion between peripheral C and H bonds. Conversely, the inter-unit torsion angles (C11–C12–C12*–C11*) were 180° and 152.8° for **3b** and **4b**, respectively, reflecting conformational flexibility around the freely rotatable C–C bonds (Fig. 3c and d). Consequently, the π-conjugated chains of **3b** and **4b** exhibited substantially different S-shaped conformations with

a C_i symmetry center and an arch-like shape with a C_2 symmetry axis, respectively, resulting in different packing motifs of the offset π-stacked arrays (Fig. 3c) and one-dimensional π-stacked columns (Fig. 3d), respectively. Nevertheless, the torsional angles in **3b** and **4b** were sufficiently small for extending π-conjugation over the main chains. Despite these conformational differences, all sp^2 carbon atoms in the biindenylidene skeletons of **3b** and **4b** maintained a planar geometry without pyramidalization. These results demonstrate that oligo(biindenylidene)s are suitable for studying the effect of five-membered rings on the electron affinity of π-conjugated hydrocarbons without the influence of the curved structure.

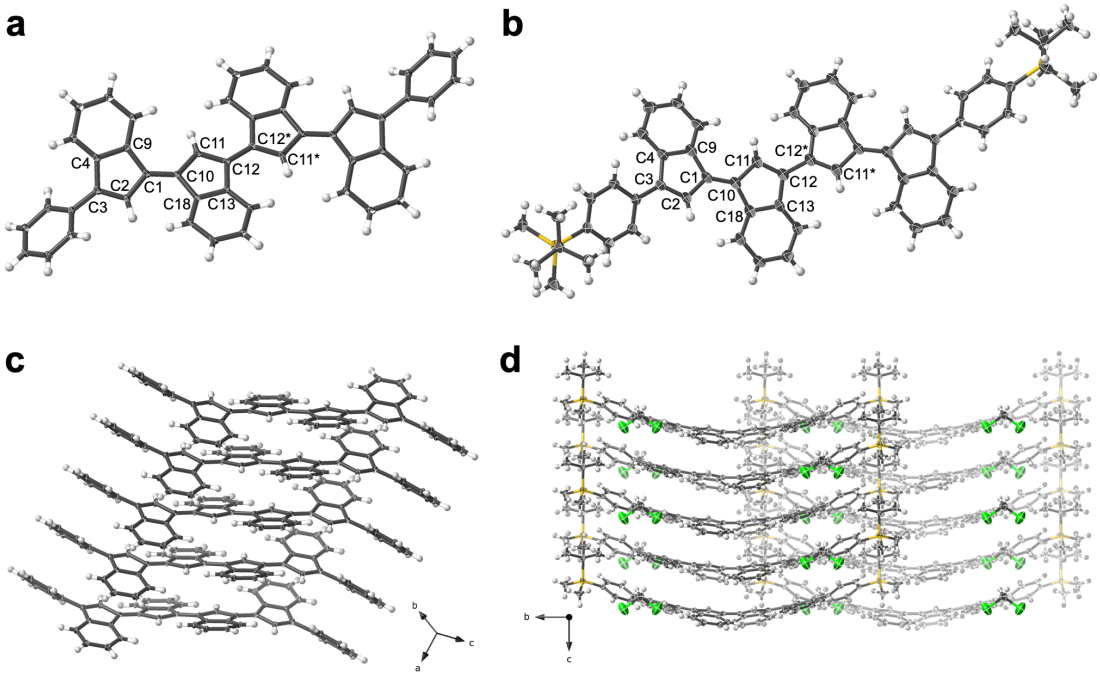

Fig. 3. X-ray crystal structures of biindenylidene dimers **3b** (a, c) and **4b** (b, d) drawn by thermal ellipsoid plots (50% probability for thermal ellipsoids): gray, carbon; white, hydrogen; yellow, silicon; green, chlorine. **a**, **b.** Top view of **3b** and **4b**. CH_2Cl_2 molecules in the crystal lattices of **4b** are omitted for clarity. **c, d.** Crystal-packing structure of **3b** and **4b**.

Electrochemical properties. To corroborate the dependence of the redox properties on the number of five-membered rings, the electrochemical properties of oligo(biindenylidene)s were examined using cyclic voltammetry. Trialkylsilylphenyl-capped biindenylidene oligomers **4a**–**c** were employed for the measurements owing to the low solubility of the phenyl-capped **3c** in tetrahydrofuran (THF). The cyclic voltammograms of **4a**, **4b**, and **4c** in THF showed two-, four-, and five-step reversible redox processes in the reductive region, respectively (Fig. 4a), and irreversible redox processes in the oxidative region (Supplementary Fig. 4). Considering that the first redox wave of **4c** was characterized by two-electron redox processes based on peak

current analyses (Supplementary Discussion 1), **4a**, **4b**, and **4c** underwent two-, four-, and six-electron reductions, respectively, within the electrochemical window of THF. These results demonstrate that oligo(biindenylidene)s can accept electrons equal to the number of five-membered rings in their main chains. Accordingly, the five-membered ring substructure ensures the prominent stability of the π-conjugated hydrocarbons toward multi-electron reduction, even without a curved structure or electron-withdrawing substituents.

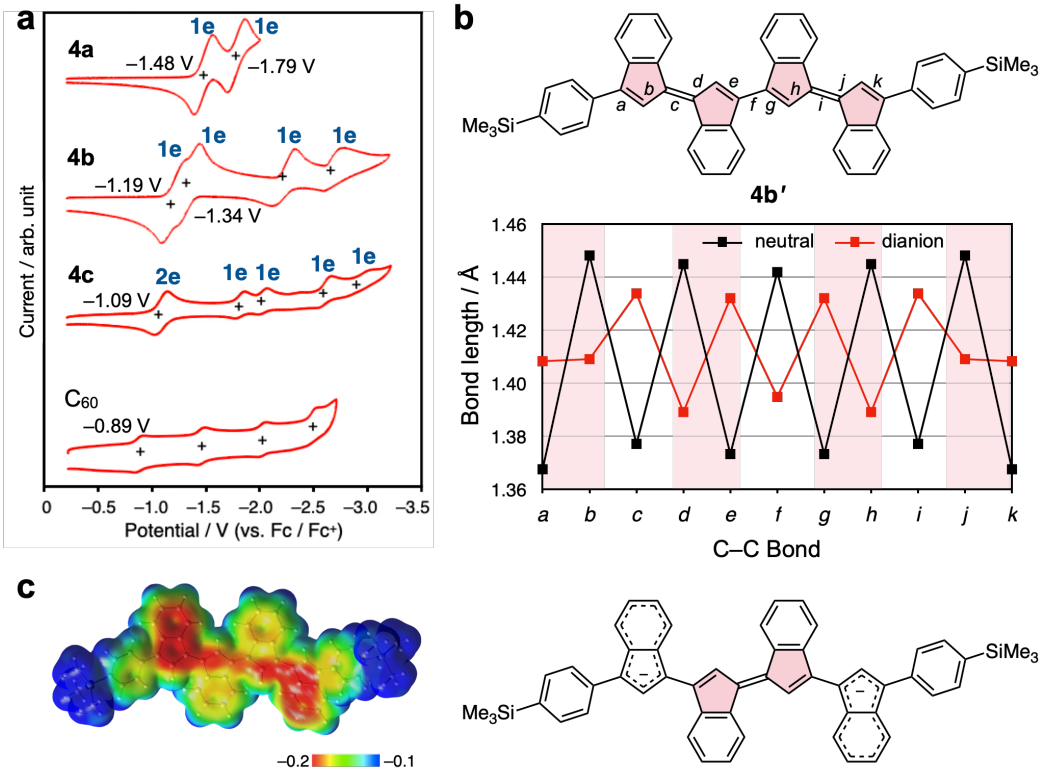

Fig. 4. Electrochemical properties of oligo(biindenylidene)s compared to those of C_{60}. **a.** Cyclic voltammograms of **4a**–**c** and C_{60} measured at a scan rate of 0.1 V s^{-1} in tetrahydrofuran using [*n*-Bu_4N][PF_6] (0.1 M) as the supporting electrolyte. All potentials are referenced against the ferrocene/ferrocenium (Fc/Fc^+) couple. **b.** Plot of selected bond lengths in the optimized geometries of **4b′** in the charge-neutral (black) and dianionic states (red) calculated at the PBE0/6-31+G(d) level of theory. **c.** Electrostatic potential map calculated at the MP2/6-31+G(d) level of theory and the proposed structure of [**4b′**]$^{2-}$.

The number of five-membered rings also gave the significant impact on the electron affinity of oligo(biindenylidene)s. Similar to those of various π-conjugated oligomers, the $E_{1/2,red1}$ values of **4a**–**c** shifted in the positive direction as the chain length increased (**4a**: –1.48 V, **4b**: –1.19 V, and **4c**: –1.09 V versus ferrocene/ferrocenium (Fc/Fc^+)), reflecting the decrease in the LUMO energy levels via the effective interaction between the π* orbitals of the biindenylidene moiety. Accordingly, the $E_{1/2,red1}$ value of **4c** was close to that of C_{60} (–0.89 V versus Fc/Fc^+),

albeit slightly more negative. This result suggests that the oligo(biindenylidene) substructure of C_{60} also plays a crucial role in its high electron affinity.

Oligo(biindenylidenes)s exhibit high electron affinity and stability toward multi-electron reduction close to fullerenes. However, electrochemical studies have also highlighted a feature of oligo(biindenylidene)s based on one-dimensional π-conjugated chains. Unlike C_{60} that undergoes multi-electron reduction in a stepwise manner with almost constant peak separations, oligo(biindenylidene)s **4** showed distinct behavior depending on the chain length. In particular, the separation of the first and second reductive waves decreased from 0.31 V (**4a**) to 0.15 V (**4b**) as the chain length increased, and these two waves merged into a single two-electron peak at **4c**. This peak separation decrease was in contrast with those of the subsequent reductive waves in **4b** and **4c**. The quantum chemical calculations of **4b′**, a model compound of **4b** wherein *t*-$BuMe_2Si$ groups were simplified to Me_3Si groups to reduce the computational costs, demonstrated the localization of charge densities in the dianionic dimer (**[4b′]**$^{2-}$) on the indenylidene skeletons at both terminals (Fig. 4c). This localization should be ascribed to the minimization of the electronic repulsion and the stabilization caused by the 10π aromaticity of the two indenyl anion moieties (Fig. 4b and c, and Supplementary Fig. 9). This charge separation in the dianion may be responsible for decreasing the peak separation of the first and second reduction waves as the chain length increases and reflects the structural feature of one-dimensional π-conjugated chains.

Electronic absorption. The ultraviolet/visible/near-infrared absorption spectra of **3** and **4** in CH_2Cl_2 were compared with that of C_{60}, highlighting the characteristics of oligo(biindenylidene)s (Fig. 5a and Supplementary Fig. 5). Similar to conventional π-conjugated oligomers, the increase in chain lengths of oligo(biindenylidene)s from **3a** to **3c** and from **4a** to **4c** resulted in a substantial redshift and an increase in the molar extinction coefficients (ε) of the longest wavelength absorption bands. In particular, the longest wavelength absorption band of phenyl-capped **3c** with an absorption maximum wavelength (λ_{max}) of 653 nm was substantially red-shifted by 171 nm (5400 cm^{-1}) compared to that of the corresponding **3a** (λ_{max} = 482 nm), and its ε value of 5.34×10^4 M^{-1} cm^{-1} also increased (**3a**: 1.32×10^4 M^{-1} cm^{-1}). Notably, all oligo(biindenylidene)s showed intense absorption bands with ε values larger than 10^4 M^{-1} cm^{-1} in the visible region, which was in contrast to the weak absorption of C_{60} ($\varepsilon < 10^3$ M^{-1} cm^{-1}) because of symmetry-forbidden transitions. In particular, the absorption spectra of **3c** and **4c** cover the entire visible region and reach the NIR region.

This pronounced light absorption of oligo(biindenylidene)s might represent a characteristic property owing to their topological difference from C_{60}. Conversely, **3a**–**c** and **4a**–**c** were virtually nonfluorescent despite the allowed nature of the $S_0 \rightarrow S_1$ transitions. Although the reason for this remains unclear, nonradiative decay processes via intersystem crossing or conical intersection may be responsible for the lack of fluorescence.

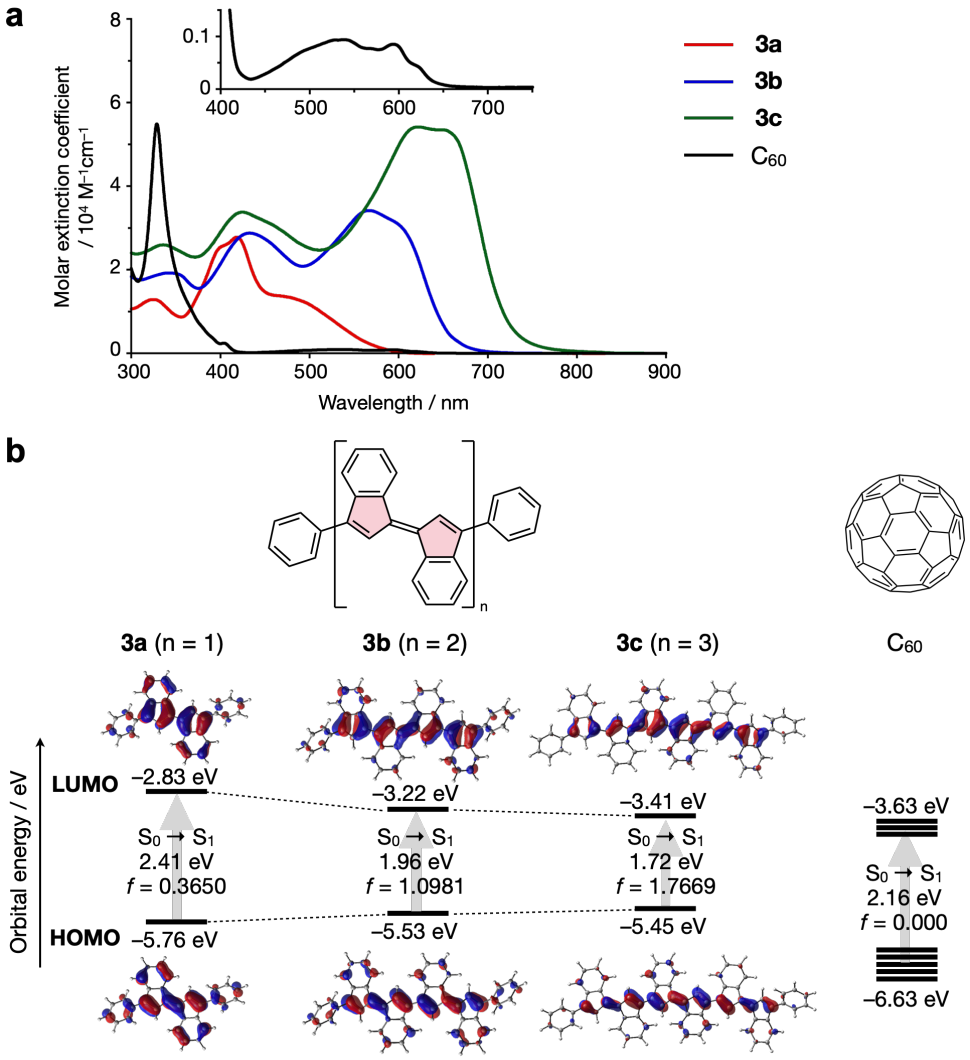

Fig. 5. Photophysical properties of oligo(biindenylidene)s compared with that of C_{60}. **a.** Ultraviolet/visible/near-infrared electronic absorption spectra of **3a–c** and C_{60} in CH_2Cl_2. Inset: magnified spectra in the wavelength range from 400–750 nm to clarify the absorption bands of C_{60}. **b.** Energy diagrams and pictorial representations of the Kohn–Sham frontier molecular orbitals for the optimized geometries of **3a–c** (C_1 symmetry) and C_{60} (I_h symmetry) and the time-dependent DFT vertical excitations for the lowest-energy transitions calculated at the PBE0/6-31+G(d) level of theory.

Time-dependent (TD) DFT calculations at the PBE0/6-31+G(d) level indicated that the highest-occupied molecular orbitals (HOMOs) and LUMOs of **3a**–**c** were characterized as

delocalized π and π* orbitals over the main chains with a negligible contribution from fused and terminal benzene rings, supporting the effective orbital interactions between the biindenylidene units (Fig. 5b and Supplementary Fig. 6). In contrast to the low-lying LUMO levels of **3a**–**c** close to C_{60}, the HOMO levels of **3a**, **3b**, and **3c** (–5.76, –5.53, and –5.45 eV, respectively) were substantially higher than that of C_{60} (–6.63 eV). These high-lying HOMO levels of **3c** are possibly responsible for the significantly narrower HOMO–LUMO gap than that of C_{60}, resulting a smaller $S_0 \rightarrow S_1$ vertical excitation energy (**3c**: 1.72 eV, C_{60}: 2.16 eV). Furthermore, the oscillator strength *f* of the $S_0 \rightarrow S_1$ transition in **3c** ($f = 1.767$) was larger than that of C_{60} ($f = 0.000$) because of its lower symmetry (Fig. 5b and Supplementary Table 3). These relatively high-lying HOMO and the symmetry-allowed characteristic of the $S_0 \rightarrow S_1$ transition in the oligo(biindenylidene)s can be attributed to polyene-like one-dimensional π-conjugation.

Conclusion

To elucidate the origin of the high electron affinity and stability toward the multi-electron reduction of fullerenes with only a carbon skeleton, we designed and synthesized end-capped **3** and **4**, which are π-conjugated hydrocarbons composed of a one-dimensional fragment of buckminsterfullerene C_{60} with the same connectivity between the five-membered rings. Crystallographic analysis of **3** and **4** confirmed that all sp^2 carbon atoms in their π-conjugated frameworks adopt trigonal planar geometries, unlike the pyramidalized carbon atoms in conventional fullerene fragment molecules. These oligo(biindenylidene)s have one-dimensional π-conjugated chains wherein the five-membered rings are directly connected. Electrochemical studies of oligo(biindenylidene)s **4** revealed that these oligo(biindenylidene)s accept electrons equal to the number of five-membered rings in their main chains and experimentally corroborated that the five-membered ring substructures play a crucial role in attaining robustness toward multi-electron reduction. Notably, oligo(biindenylidene)s, which are small-molecule π-conjugated hydrocarbons that do not have a rigid structure or curvature like fullerenes, can accept up to six electrons without noticeable decomposition.

In contrast to the similarity with fullerenes in terms of electron affinity, the one-dimensional π-conjugation in oligo(biindenylidene)s resulted in pronounced absorption covering the entire visible region, unlike the weak absorption of C_{60} attributable to the highly symmetrical structure. The current results highlight the significance of the pentagonal substructure for attaining

stability toward multi-electron reduction and provide a new strategy for the molecular design of electron-accepting π-conjugated hydrocarbons.

Data availability

The crystallographic data (CIF files) of **3a**, **3b**, **4a**, **4b**, **6a**, **7a**, and **8** have been deposited with the Cambridge Crystallographic Data Centre (CCDC) as supplementary publications; CCDC 2184328–2184334 contain the supplementary crystallographic data. These data can be obtained free of charge from CCDC at [www.ccdc.cam.ac.uk/data_request/cif]. All other data generated or analyzed during the study are available in this article and its Supplementary Information files.

References

1. Kroto, H. W., Heath, J. R., O'Brien, S. C., Curl, R. F. & Smalley, R. E. C_{60}: Buckminsterfullerene. *Nature* **318**, 162–163 (1985).
2. Xie, Q., Perez-Cordero, E. & Echegoyen, L. Electrochemical detection of C_{60}^{6-} and C_{70}^{6-}: Enhanced stability of fullerides in solution. *J. Am. Chem. Soc.* **114**, 3978–3980 (1992).
3. Chabre, Y. *et al.* Electrochemical intercalation of lithium into solid fullerene C_{60}. *J. Am. Chem. Soc.* **114**, 764–766 (1992).
4. Ganin, A. Y. *et al.* Bulk superconductivity at 38 K in a molecular system. *Nat. Mater.* **7**, 367–371 (2008).
5. Takabayashi, Y. *et al.* The Disorder-Free Non-BCS Superconductor Cs_3C_{60} Emerges from an Antiferromagnetic Insulator Parent State. *Science* **323**, 1585–1590 (2009).
6. Ganin, A. Y. *et al.* Polymorphism control of superconductivity and magnetism in Cs_3C_{60} close to the Mott transition. *Nature* **466**, 221 (2010).
7. Wang, L.-S., Conceicao, J., Jin, C. & Smalley, R. E. Threshold photodetachment of cold C_{60}^-. *Chem. Phys. Lett.* **182**, 5–11 (1991).
8. Allemand, P. *et al.* Two different fullerenes have the same cyclic voltammetry. *J. Am. Chem. Soc.* **113**, 1050–1051 (1991).
9. Akaike, K. *et al.* Ultraviolet photoelectron spectroscopy and inverse photoemission spectroscopy of [6,6]-phenyl-C_{61}-butyric acid methyl ester in gas and solid phases. *J. Appl. Phys.* **104**, 023710 (2008).
10. Haddon, R. C. *et al.* C_{60} thin film transistors. *Appl. Phys. Lett.* **67**, 121–123 (1995).
11. Li, H. *et al.* High-Mobility Field-Effect Transistors from Large-Area Solution-Grown Aligned C_{60} Single Crystals. *J. Am. Chem. Soc.* **134**, 2760–2765 (2012).
12. Zhang, Y., Murtaza, I. & Meng, H. Development of fullerenes and their derivatives as

semiconductors in field-effect transistors: exploring the molecular design. *J. Mater. Chem. C* **6**, 3514–3537 (2018).

13. Bao, Z., Lovinger, A. J. & Brown, J. New air-stable n-channel organic thin film transistors. *J. Am. Chem. Soc.* **120**, 207–208 (1998).
14. Facchetti, A., Yoon, M., Stern, C. L., Katz, H. E. & Marks, T. J. Building blocks for n-Type organic electronics: regiochemically modulated inversion of majority carrier sign in perfluoroarene-modified polythiophene semiconductors. *Angew. Chem. Int. Ed.* **42**, 3900–3903 (2003).
15. Schmidt, R. *et al.* High-performance air-stable n-channel organic thin film transistors based on halogenated perylene bisimide semiconductors. *J. Am. Chem. Soc.* **131**, 6215–28 (2009).
16. Acker, D. S. & Hertler, W. R. Substituted quinodimethans. I. preparation and chemistry of 7,7,8,8-tetracyanoquinodimethan. *J. Am. Chem. Soc.* **84**, 3370–3374 (1962).
17. Usta, H. *et al.* Design, synthesis, and characterization of ladder-type molecules and polymers. Air-stable, solution-processable n-channel and ambipolar semiconductors for thin-film transistors via experiment and theory. *J. Am. Chem. Soc.* **131**, 5586–5608 (2009).
18. Lin, Y. *et al.* An electron acceptor challenging fullerenes for efficient polymer solar cells. *Adv. Mater.* **27**, 1170–1174 (2015).
19. Tang, C. W. Two-layer organic photovoltaic cell. *Appl. Phys. Lett.* **48**, 183–185 (1986).
20. Haddon, R. C. Electronic structure, conductivity and superconductivity of alkali metal doped C_{60}. *Acc. Chem. Res.* **25**, 127–133 (1992).
21. Fowler, P. W. & Ceulemans, A. Electron Deficiency of the Fullerenes. *J. Phys. Chem.* **99**, 508–510 (1995).
22. Barth, W. E. & Lawton, R. G. Dibenzo[*ghi,mno*]fluoranthene. *J. Am. Chem. Soc.* **88**, 380–381 (1966).
23. Sygula, A. & Rabideau, P. W. A practical, large scale synthesis of the corannulene system. *J. Am. Chem. Soc.* **122**, 6323–6324 (2000).
24. Sakurai, H., Daiko, T. & Hirao, T. A Synthesis of sumanene, a fullerene fragment. *Science* **301**, 1878 (2003).
25. Abdourazak, A. H., Sygula, A. & Rabideau, P. W. "Locking" the bowl-shaped geometry of corannulene: cyclopentacorannulene. *J. Am. Chem. Soc.* **115**, 3010–3011 (1993).
26. Cronstein, H. E., Choi, N. & Scott, L. T. Practical Synthesis of an Open Geodesic Polyarene with a Fullerene-type 6:6-Double Bond at the Center: Diinedno[1,2,3,4-*defg*;1′,2′,3′,4′-*mnop*]chrysene. *J. Am. Chem. Soc.* **124**, 8870–8875 (2002).
27. Rabideau, P. W. *et al.* Buckybowls: Synthesis and ab initio calculated structure of the first

semibuckminsterfullerene. *J. Am. Chem. Soc.* **116**, 7891–7892 (1994).

28. Scott, L. T., Bratcher, M. S. & Hagen, S. Synthesis and characterization of a $C_{36}H_{12}$ fullerene subunit. *J. Am. Chem. Soc.* **118**, 8743–8744 (1996).
29. Wu, T.-C., Hsin, H.-J., Kuo, M.-Y., Li, C.-H. & Wu, Y.-T. Synthesis and structural analysis of a highly curved buckybowl containing corannulene and sumanene fragments. *J. Am. Chem. Soc.* **133**, 16319–16321 (2011).
30. Tanaka, Y., Fukui, N. & Shinokubo, H. *as*-Indaceno[3,2,1,8,7,6-*ghijklm*]terrylene as a near-infrared absorbing C_{70}-fragment. *Nat. Commun.* **11**, 3873 (2020).
31. Brunetti, F. G., Varotto, A., Batara, N. A. & Wudl, F. "Deconvoluted fullerene" derivatives: synthesis and characterization. *Chem. Eur. J.* **17**, 8604–8608 (2011).
32. Iwamoto, T., Watanabe, Y., Sakamoto, Y., Suzuki, T. & Yamago, S. Selective and random syntheses of [*n*]cycloparaphenylenes (*n* = 8–13) and size dependence of their electronic properties. *J. Am. Chem. Soc.* **133**, 8354–8361 (2011).
33. Segawa, Y. *et al.* Combined experimental and theoretical studies on the photophysical properties of cycloparaphenylenes. *Org. Biomol. Chem.* **10**, 5979–5984 (2012).
34. Wennerstroem, O. Qualitative evaluation of the band gap in polymers with extended π systems. *Macromolecules* **18**, 1977–1980 (1985).
35. Hong, S. Y. & Lee, K. W. Small band-gap polymers: quantum-chemical study of electronic structures of degenerate π-conjugated systems. *Chem. Mater.* **12**, 155–160 (2000).
36. Hong, S. Y. Zero band-gap polymers: quantum-chemical study of electronic structures of degenerate π-conjugated systems. *Chem. Mater.* **12**, 495–500 (2000).
37. Hong, S. Y. & Kim, S. C. Towards Designing Environmentally Stable Conjugated Polymers with very Small Band-Gaps. *Bull. Korean Chem. Soc.* **24**, 1649–1654 (2003).
38. Hori, Y., Nagano, Y., Uchiyama, H., Yamada, Y. & Taniguchi, H. Bromination of active hydrogen compounds by bromotrichloromethane and 1,8-diazabicyclo [5.4.0]undecene-7. A convenient synthesis for bromides and olefins. *Chem. Lett.* **7**, 73–76 (1978).
39. Priebsch, W., Hoch, M. & Rehder, D. Ringhalogenierte carbonyl(η^5-cyclopentadienyl)vanadium-komplexe. *Chem. Ber.* **121**, 1971–1975 (1988).
40. Ruoff, R. S., Tse, D. S., Malhotra, R. & Lorents, D. C. Solubility of C_{60} in a variety of solvents. *J. Phys. Chem.* **97**, 3379–3383 (1993).

Acknowledgements

The authors thank the iCeMS Analysis Center for providing access to the NMR spectrometer. The authors are grateful to Prof. Susumu Kitagawa (Kyoto University) for providing access to the X-ray diffractometer. Mass spectrometry experiments were carried out at the MS Section in the Institute for Chemical Research, Kyoto University. Synchrotron X-ray crystallography experiments were performed at the BL02B1 beamline of SPring-8, with the approval of the Japan Synchrotron Radiation Research Institute (JASRI; Project No. 2019A1057, 2019B1129, 2019B1784, 2020A0557, 2020A1056, 2020A1644, 2020A1650, 2020A1656, 2021A1578, 2021A1592, 2021B1435, 2021B1798, 2021B1833, and 2022A1705). This research was funded by a Grant-in-Aid for Scientific Research (B) (JSPS KAKENHI Grant Number 21H01916), Grant-in-Aid for Transformative Research Areas (A) "Condensed Conjugation" (JSPS KAKENHI Grant Number JP20H05864) from MEXT, Japan, and research promotion grant from the Kyoto University Foundation (A.F.). M.H thanks JSPS for the Research Fellowship for Young Scientists.

Author contributions

A.F. conceived the concept. A.T. explored the initial synthetic route. M.H. and N.S. performed the synthesis and characterization. S.T. assisted with synthesis and characterization. M.H. conducted crystallographic analysis and quantum chemical calculations. M.H. and A.F. prepared the manuscript. S.Y. proofread it. A.F. directed the project.

Competing interests

The authors declare no competing interests.

ORCID for corresponding authors

Aiko Fukazawa: 0000-0002-2903-105X

Supplementary Information

Experimental procedures and characterization data. Supplementary discussions 1–3, Figs. 1–42, Tables 1–14, and references 1–6.